# Energy Confinement of Lower-Hybrid-Current–Driven Tokamak Plasmas

S. Knowlton, M. Porkolab, Y. Takase, S. Texter, P. Bonoli, C. Fiore, S. McCool,[a] F. S. McDermott, and J. L. Terry

*Plasma Fusion Center, Massachusetts Institute of Technology, Cambridge, Massachusetts 02139*

(Received 30 January 1986)

The energy content of high-density, purely lower-hybrid-current–driven plasmas has been measured under a variety of operating conditions on the Alcator-C tokamak. The energy stored in the current-carrying electron tail can be a large fraction of the total kinetic energy in an rf-driven plasma, while the energy residing in the bulk plasma is comparable to that of a similar Ohmic discharge. At densities $\bar{n}_e \leqslant 3\times10^{13}$ cm$^{-3}$, the global confinement time of the rf-driven plasma is similar to that of an Ohmic plasma, but degrades relative to its Ohmic counterpart at higher densities and/or rf powers.

PACS numbers: 52.50.Gj, 52.35.Hr, 52.55.Fa, 52.55.Pi

Tokamak plasma currents sustained completely by lower hybrid rf current drive have been achieved in a number of experiments.[1] Experimental findings have supported the basic predictions of the Fisch theory[2]: The rf-driven current is carried by a superthermal electron tail in the distribution function, and the rf power required to maintain this tail current is proportional to the density and plasma current. On Alcator-C, an empirical current-drive efficiency, defined as $\eta = \bar{n}_e I_p R_0/P_{\rm rf}(10^{20}$ m$^{-2}$ MA MW$^{-1}$), of $\eta = 0.12$ has been measured for densities up to $\bar{n}_e = 1\times10^{14}$ cm$^{-3}$.[3] Here, $\bar{n}_e$ is the line-averaged electron density, $I_p$ is the plasma current, $R_0$ is the plasma major radius, and $P_{\rm rf}$ is the net injected rf power. The density scaling of the current-drive efficiency is in agreement with the theoretical supposition that the major loss of the superthermal electrons is due to collisions with bulk electrons; i.e., that tail energy is transformed primarily into plasma thermal energy. Regarding the overall energy confinement of such plasmas, it is important to note that rf current-driven plasmas represent auxiliary-heated discharges in which the plasma is maintained and heated entirely by non-Ohmic power. In this Letter, we present measurements of the energy content and global energy-confinement times of rf-driven plasmas and compare them with measurements in similar Ohmic plasmas. Energy-confinement studies of lower-hybrid-current–driven discharges at low densities ($\bar{n}_e \lesssim 10^{13}$ cm$^{-3}$) have also been reported recently from the PETULA-B[4] and ASDEX[5] tokamaks. In the present study, however, experiments have been performed in a reactor-relevant regime at densities up to $\bar{n}_e = 8\times10^{13}$ cm$^{-3}$.

The confinement experiments were performed on the Alcator-C tokamak ($R_0 = 64$ cm, $a = 16.5$ cm) in the parameter range $\bar{n}_e = (2\text{–}8)\times10^{13}$ cm$^{-3}$, $B = 7\text{–}11$ T, $I_p = 100\text{–}200$ kA, $q(a) > 8$, $Z_{\rm eff} = 1.5\text{–}2$, and $P_{\rm rf} \lesssim 1.0$ MW at $f = 4.6$ GHz in hydrogen discharges with molybdenum limiters. Electron temperature profiles were measured with a five-channel Thomson scattering system and the central ion temperature was determined by charge-exchange analysis. Plasmas of constant current were maintained by injection of sufficient rf power into Ohmically created target plasmas; during the rf current-drive phase, no current flowed in the Ohmic primary circuit and the loop voltage was reduced to zero. Following temperature measurements on rf-driven plasmas, conventional Ohmic discharges of idential current and density were studied in order to make comparisons under as similar conditions as possible.

The results of a typical comparison are shown in Fig. 1. The evolution of the current, loop voltage, density, central electron temperature, and equilibrium quantity $\beta_p + l_i/2$ are illustrated for both an rf current-driven and an Ohmic discharge. For the rf-driven plasma, the loop voltage is zero, $I_p = 135$ kA, $\bar{n}_e = 4\times10^{13}$ cm$^{-3}$, and the rf power is 460 kW; for the corresponding Ohmic discharge, the Ohmic power is 200 kW. Within experimental error, the central temperatures of both the Ohmic and rf-driven plasmas are the same, and the electron-temperature profile widths are also very similar; consequently the thermal energy contents of the two discharges [$W_e^{\rm bulk}({\rm rf}) \simeq W_e^{\rm bulk}({\rm Oh}) = 1.4$ kJ] are nearly identical. The observed increase of $\beta_p + l_i/2$ in the rf-driven plasma relative to that of the Ohmic plasma is attributed to the kinetic energy stored in the current-carrying superthermal electron tail of the former. This conclusion is supported by measurements of the plasma hard x-ray emission spectrum ($E_\gamma = 30\text{–}500$ keV) performed with an eight-channel vertically viewing array and a five-channel array which views the plasma at different angles with respect to the toroidal field.[6] Using the techniques of von Goeler *et al.*,[7] we have modeled the two-dimensional shape of the fast-electron distribution function from x-ray measurements taken at a density of $\bar{n}_e = 3\times10^{13}$ cm$^{-3}$ and a current of $I_p = 140$ kA. Since the loop voltage is

 

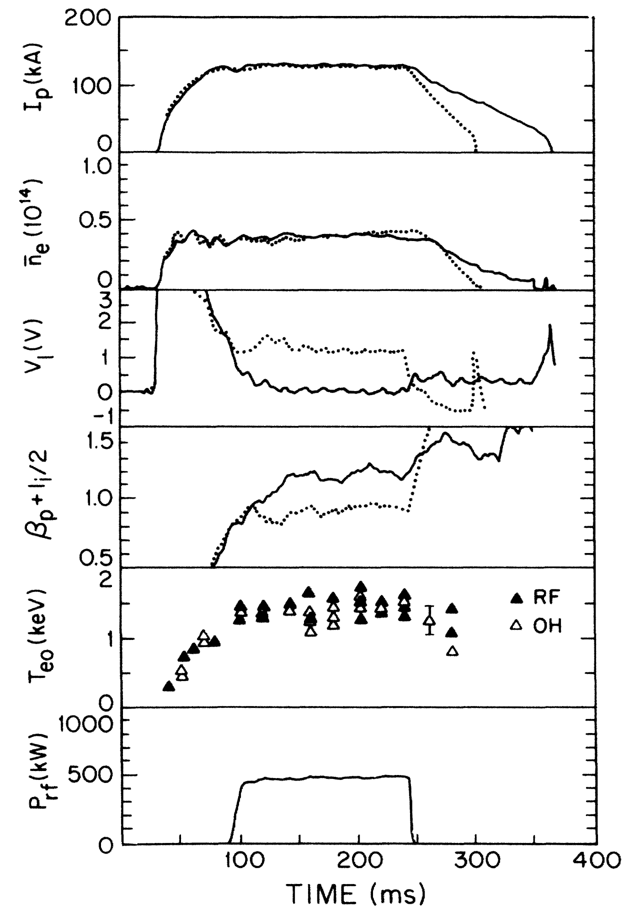


FIG. 1. Comparison of the plasma-parameter time histories of an rf-driven discharge (solid lines) and an Ohmic discharge (dotted lines) for $B=8$ T. From top to bottom: plasma current, line-averaged density, loop voltage, $\beta_p + l_i/2$, central electron temperature obtained on a shot-by-shot basis, and rf power.

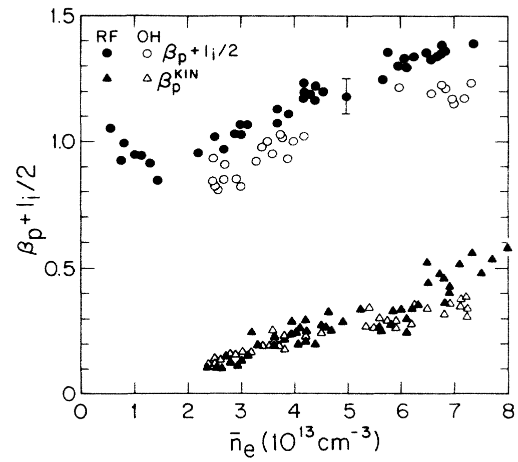


FIG. 2. $\beta_p$ and $\beta_p + l_i/2$ vs density for rf-driven and Ohmic plasmas for $I_p \simeq 140$ kA, $B=8$ T. Triangles represent kinetic $\beta_p$ measurements (Thomson scattering and charge exchange), while the circles depict equilibrium field measurements.

zero, it is reasonable to assume that the entire plasma current is carried by the electron tail; therefore, the macroscopic parameters of the tail can be calculated.[7] In particular, the fractional density of the tail relative to the bulk is 0.7%, and the energy moment over the tail distribution gives a value of $1.4 \pm 0.3$ kJ, with the estimated error arising primarily from the ambiguity in the modeling of the fast-electron distribution.

The variation of $\beta_p$ with density is shown in Fig. 2 for plasma currents of $I_p \simeq 140$ kA and a toroidal magnetic field of $B=8$ T. The triangles at the bottom of the graph represent the values of $\beta_p$ calculated from kinetic measurements of the bulk plasma. Up to a density of $\bar{n}_e = 6\times10^{13}$ cm$^{-3}$, the bulk stored energy of the Ohmic and rf-driven plasmas is similar, while at higher densities some additional heating of the bulk plasma is occurring in the rf-driven case. Over the range of densities illustrated in the figure, the input power to the Ohmic discharges remained at $P_{\rm Oh} \simeq 200$ kW. To perform the density scan for the purely rf-driven plasmas, the rf power was raised from $P_{\rm rf} = 200$ kW at $\bar{n}_e = 1.5\times10^{13}$ cm$^{-3}$ to $P_{\rm rf} = 950$ kW at $\bar{n}_e = 8\times10^{13}$ cm$^{-3}$ in order to keep the current constant. The data points at the top of the graph indicate the measurements of $\beta_p + l_i/2$ from the equilibrium measurements. Though the absolute level of the magnetic $\beta_p + l_i/2$ measurement is too low (based on the kinetic measurements) because of base-line errors, comparisons of relative values remain valid. We note that the measured $\beta_p + l_i/2$ in rf-driven plasmas is always higher than in their Ohmic counterparts. For the case in which the tail was measured by hard x-ray spectrometry ($\bar{n}_e \simeq 3\times10^{13}$ cm$^{-3}$), the difference in $\beta_p + l_i/2$ between the Ohmic and rf-driven cases is approxiamately 0.18, which corresponds to $W_e^{\rm tail} \simeq 0.9$ kJ. In the deduction of this value, the equilibrium field measurement was corrected for the pressure anisotropy of the tail[8] and $l_i/2$ was assumed to be unchanged from the Ohmic case. The magnitude of the tail energy estimated in this fashion is in the same range as that from the x-ray measurements. The difference in the two may be attributed to experimental error and a possible lowering of the internal inductance in the rf-driven plasma relative to the Ohmic one. In rf-driven plasmas, the current profile cannot necessarily be computed from the temperature profile; in fact, in recent ASDEX experiments, the temperature profile was found to narrow during rf current drive while the current profile broadened slightly.[9] If we assume that the same fractional change in inductance occurs in our experiment as in ASDEX, the tail energy increases by approximately 20% above our previous estimate and the total stored energy by approximately 10%. In subsequent calculations of the plasma

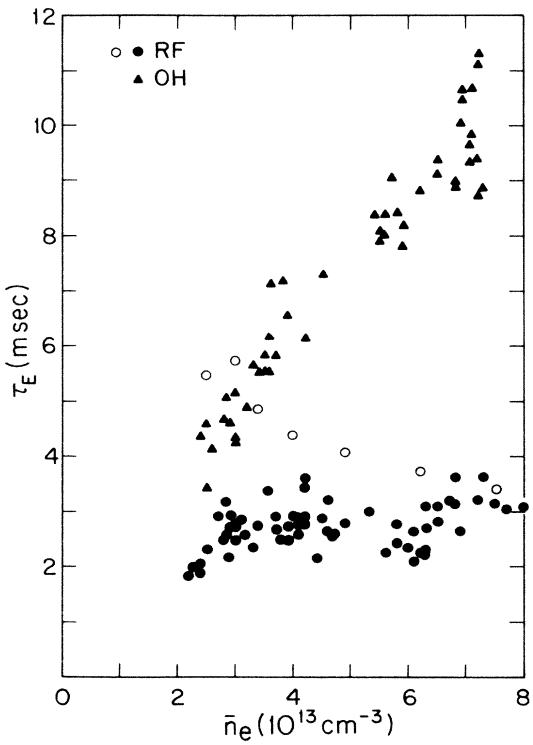


FIG. 3. Global energy-confinement time of rf-driven and Ohmic plasmas vs density. The solid circles represent the quantity $W^{bulk}/P_{rf}$ calculated for the rf-driven plasmas.

energy content, the internal inductance is taken to be the same for rf and Ohmic plasmas over the density scan, which may result in the energy in the tail being underestimated.

The global energy-confinement times for both the rf-driven and Ohmic plasmas are shown in Fig. 3 as functions of density. The confinement time in these quasi steady-state discharges is defined as $\tau_E = W^{tot}/P_{in}$, where $W^{tot}$ is the total stored energy in the electron and ion populations (including the electron tail) and $P_{in}$ is the net input power to the plasma. For the rf-driven plasmas, we have used the net transmitted rf power for $P_{in}$. We may add that experimental measurements of the current-drive efficiency suggest that the absorbed fraction of rf power does not vary strongly over the density range of our experiment. Moreover, code simulations of Alcator-C current-driven plasmas which successfully reproduce the experimental current-drive efficiencies suggest that over 95% of the injected rf power is absorbed by electron Landau damping.[10]

The global energy-confinement time of the Ohmic plasmas increases linearly with density, as expected from neo-Alcator scaling.[11] However, the confinement of the rf-driven plasmas shows a decreasing trend with density and/or power. Shown by solid circles are the calculated confinement times of the rf-driven plasmas if only the bulk energy is taken into account, as in the case of Ohmic plasmas. These values are not to be taken as good estimates of the true bulk confinement times because of the possibility of radial loss of tail electrons. The difference between these calculated values and the true global confinement time $\tau_E$ (shown in open circles) defined earlier indicates the importance of the stored tail energy in the overall energy balance. At densities $\bar{n}_e \leq 3\times 10^{13}$ cm$^{-3}$, the global confinement times of the rf-driven plasmas are similar to and may even exceed that of the Ohmic plasmas because of the presence of the energetic electron tail. As the density (and rf power) are raised, the rf confinement time degrades relative to the Ohmic value, and the tail energy represents an increasingly smaller fraction of the total plasma energy content. The decreasing trend of confinement time with injected power is similar to Kaye-Goldston scaling for neutral-beam-heated $L$-mode plasmas.[12] Comparisons of Ohmic and rf confinement times have also been made as functions of the plasma current and toroidal field. As the current is raised from $I_p = 100$ to 200 kA, $\tau_E^{Oh}$ decreases by 25%, while $\tau_E^{rf}$ increases by approximately the same fraction because of an increase in the estimated tail energy with plasma current. The value of $\tau_E^{rf}$ increases by at most 20% as the toroidal field is raised from $B_T = 7$ to 11 T, with $\tau_E^{Oh}$ remaining constant over the same range. The major difference in the confinement properties of the two types of discharges appears to be the unfavorable density dependence of $\tau_E^{rf}$ relative to Ohmic plasmas, or degraded confinement with increased total input power.

The impurity behavior was monitored in some of these experiments to assess the role of radiation in the power balance of current-driven plasmas. Spectroscopic measurements of the light-impurity (C,O) emissions indicated that their densities were unchanged or increased by at most a factor of 2 during rf injection. Molybdenum emissions increased between a factor of 5 and 15, while the bolometer signal increased by roughly a factor of 5 during rf injection. The radiated power as measured by the bolometer, and inferred from the molybdenum line brightnesses, was observed to decrease with increasing density. The $Z_{eff}$ measured by visible bremsstrahlung showed a similar trend. The absolute calibration of the bolometer is presently in some doubt; however, the total fraction of radiated power due to high-$Z$ impurities based on spectroscopic measurements and the cooling rates of Post *et al.*[13] was estimated to be $P_{rad}/P_{rf} \lesssim 0.15$ at the highest powers employed in this experiment. Although the radiation levels are strongly enhanced during rf injection, radiation appears to play a less important role in the overall power balance of the rf driven plasma as the density and rf power are raised, and therefore does not explain the diverging trend in $\tau_E^{rf}$

and $\tau_E^{Oh}$ at the higher densities.

In order to investigate other possible reasons for the different scaling in the confinement times, we have simulated these discharges with a detailed Fokker-Planck–ray-tracing-transport code.[10] The radial loss time for fast electrons is taken to be a constant (3 msec) multiplied by a velocity-dependent factor.[14] The bulk electron thermal conductivity $\chi_e$ is modeled in both Ohmic and rf discharges by Coppi-Mazzucato diffusion[15]; in the latter case, we allow $\chi_e$ to be multiplied by an adjustable factor to match the experimentally obtained temperatures. As mentioned earlier, this code models the macroscopic parameters and current-drive efficiency of rf-driven discharges with fair accuracy. For the simulations of the Alcator-C experiments, the main energy loss of the current-carrying fast electrons was found to be collisional absorption on the bulk. Radial losses of tail electron energy were approximately one-third of the input rf power at a density of $\bar{n}_e = 3\times10^{13}$ cm$^{-3}$, but only one-sixth of the input power at $\bar{n}_e = 7\times10^{13}$ cm$^{-3}$. If the confinement time of the tail electrons (typically 4–6 msec) was significantly reduced, flat-top current drive could not be maintained in the simulations with the experimentally given input powers. Although the rf deposition profiles are predicted to be broader than Ohmic ones, almost all the rf power is calculated to be absorbed inside $r/a = 0.4$ for all densities in this experiment. Thus, the apparent degradation in confinement relative to the Ohmic plasma is not explained by either unfavorable rf power deposition profiles or poor confinement of the superthermal electrons. To attain similar bulk temperatures in the code to those observed experimentally, it was necessary to increase $\chi_e$ in the rf-driven plasma above that of the Ohmic plasma at higher densities; an acceptable match of the simulation and experiment could be achieved by setting $\chi_e^{rf} = \chi_e^{Oh}$ at $\bar{n}_e = 3\times10^{13}$ cm$^{-3}$ and $\chi_e^{rf} = 2.3\chi_e^{Oh}$ at $\bar{n}_e = 7\times10^{13}$ cm$^{-3}$. Thus a plausible explanation of our experimental results is that the confinement of the thermal component of the rf-driven plasma degrades relative to that of the Ohmic plasma with increasing density. This finding is consistent with $\chi_e^{rf}$ remaining nearly independent of density, or increasing with increasing total input power.

In summary, the energy content of purely lower-hybrid-current–driven plasmas has been compared with that of Ohmic plasmas. The bulk plasma energies of the two types of discharges are found to be similar over a wide range of parameters. In rf-driven discharges, a significant amount of additional kinetic energy resides in the superthermal electron tail. Under plausible assumptions of the rf absorption efficiency, the global energy-confinement time is found to be lower in rf current-driven plasmas than in Ohmic ones for densities $\bar{n}e \gtrsim 3\times10^{13}$ cm$^{-3}$.

We thank Mr. David Griffin for his tireless rf engineering support, and the Alcator-C technical and professional staff for their many contributions to this experiment. This work was supported by the U.S. Department of Energy under Contract No. DE-AC02-78ET51013.

[a]Present address: University of Texas, Austin, TX 78712.

[1]For recent reviews of lower-hybrid-current–drive experiments, see W. Hooke, Plasma Phys. Controlled Fusion **26**, 133 (1984); M. Porkolab, in *Wave Heating and Current Drive in Plasmas,* edited by V. L. Granatstein and P. L. Colestock (Gordon and Breach, New York, 1985), p. 219.

[2]N. J. Fisch, Phys. Rev. Lett. **41**, 873 (1978); C. F. F. Karney and N. J. Fisch, Phys. Fluids **22**, 1817 (1979).

[3]M. Porkolab *et al.*, Phys. Rev. Lett. **53**, 450 (1984).

[4]C. Gormezano *et al.*, in *Radiofrequency Plasma Heating,* edited by D. Gary Swanson, AIP Conference Proceedings No. 129 (American Institute of Physics, New York, 1985), p. 111.

[5]F. Sölnder *et al.*, in *Proceedings of the Twelfth European Conference on Controlled Fusion and Plasmas Physics, Budapest, Hungary, 1985,* edited by L. Pócs and A. Montvai (European Physical Society, Petit Lancy, Switzerland, 1985), Vol. 2, p. 244.

[6]S. Texter *et al.*, Massachusetts Institute of Technology Plasma Fusion Center Report No. PFC/JA-86-10, 1986 (unpublished); S. Texter, Ph.D. thesis, Massachusetts Institute of Technology, 1986, Massachusetts Institute of Technology Plasma Fusion Center Report No. PFC/RR-85-24, 1986 (unpublished).

[7]S. von Goeler *et al.*, Nucl. Fusion **25**, 1515 (1985); J. Stevens *et al.*, Nucl. Fusion **25**, 1529 (1985).

[8]A. Mondelli and E. Ott, Phys. Fluids **17**, 1017 (1974).

[9]K. McCormick *et al.*, in Ref. 5, Vol. 1, p. 199.

[10]P. Bonoli, R. Englade, and M. Porkolab, in *Proceedings of the Fourth International Symposium on Heating in Toroidal Plasmas, Rome, Italy, 1984,* edited by H. Knoepfel and E. Sindoni (International School of Plasma Physics, Varenna, Italy, 1984), Vol. 2, p. 1311; P. Bonoli and R. Englade, Massachusetts Institute of Technology Plasma Fusion Center Report No. PFC/JA-86-5, 1986 (to be published).

[11]B. Blackwell *et al.*, in *Proceedings of the Ninth International Conference on Plasma Physics and Controlled Nuclear Fusion Research, Baltimore, Maryland, 1982* (International Atomic Energy Agency, Vienna, Austria, 1983), Vol. 2, p. 27.

[12]S. M. Kaye and R. J. Goldston, Nucl. Fusion **25**, 65 (1985); S. M. Kaye, Phys. Fluids **28**, 2327 (1985).

[13]D. E. Post *et al.*, At. Data Nucl. Data Tables **20**, 397 (1977).

[14]H. E. Mynick and J. D. Strachan, Phys. Fluids **24**, 695 (1981).

[15]B. Coppi and E. Mazzucato, Phys. Lett. **71A**, 337 (1979).